Article

Tannins as Biobased Molecules for Surface Treatments of Flax Wrapped Rovings for Epoxy/Flax Fabrics Biocomposites: Influence on Mechanical Properties through a Multi-Scale Approach

Khouloud Tilouche-Guerdelli [1], Clément Lacoste [1,*], Didier Perrin [1], Pierre-Jacques Liotier [1], Pierre Ouagne [2], Jacopo Tirillò [3], Fabrizio Sarasini [3] and Anne Bergeret [1,*]

[1] Polymers Composites and Hybrids (PCH), IMT Mines Ales, 30100 Ales, France; khouloud.tilouche@mines-ales.fr (K.T.-G.); didier.perrin@mines-ales.fr (D.P.); pierre-jacques.liotier@mines-ales.fr (P.-J.L.)

[2] Laboratoire Génie de Production (LGP), Université de Toulouse, INP-ENIT, 65016 Tarbes, France; pierre.ouagne@enit.fr

[3] Department of Chemical Engineering Materials Environment, Sapienza-Università di Roma, 00184 Roma, Italy; jacopo.tirillo@uniroma1.it (J.T.); fabrizio.sarasini@uniroma1.it (F.S.)

[*] Correspondence: clement.lacoste@mines-ales.fr (C.L.); anne.bergeret@mines-ales.fr (A.B.)

Abstract: The present study examined the effect of biobased molecules grafted onto wrapped flax rovings on the mechanical properties of fabrics designed for epoxy-based biocomposites, aiming to optimize fiber/matrix adhesion. Biobased solutions, such as tannins from quebracho, were used to treat wrapped flax rovings in comparison to a non-biobased aminosilane solution used as a reference. The chemical treatment is performed using an innovative lab-scale impregnation line. The influence of the solution concentration has been investigated. SEM-EDX and FT-IR confirmed the grafting efficiency of molecules on wrapped rovings. Plain and 5-harness satin fabrics were then manufactured at lab scale with the resulting functionalized rovings. Tensile tests were carried out on rovings and on fabrics. A concentration of 1% silane is sufficient to improve the mechanical properties of rovings and fabrics. The addition of NaOH to tannins strengthens flax fiber rovings more than tannins alone, and the weave pattern influences mechanical performance.

Keywords: wrapped flax rovings; weaving; flax fabrics; quebracho tannins; impregnation line; mechanical properties

1. Introduction

Most composite materials are currently produced using non-renewable reinforcing materials, such as glass, carbon, and aramid fibers. But growing environmental awareness has nowadays driven efforts to develop composite materials reinforced by lignocellulosic fibers such as flax, hemp, jute, kenaf, and sisal fibers [1–6]. As mentioned by Rangappa and Siengchin [7] in their article, they offer an in-depth analysis of lignocellulosic fibers, and their use as reinforcements in biocomposites. They highlight many new prospects and potentials for plant fibers to serve as alternatives to conventional fibers such as glass fibers, helping to strengthen their market position. These biocomposites represent challenging alternatives due to their versatile properties, such as low density, great specific mechanical properties, low cost, and environmental benefits [8–11] even if their fire resistance and hydrophilicity need to be challenged. The mechanical properties of biocomposites depend mainly on the nature of the reinforcing fibers, on the fiber volume fraction, on their architecture (short fiber, non-woven yarns, rovings, unidirectional preforms, woven fabrics, etc.), and on their manufacturing technique (infusion, extrusion, injection molding,

thermocompression molding, resin transfer molding (RTM)) [11]. Flax fibers are of particular interest, and many studies and some reviews focus on their competitiveness and their ability to reinforce polymer matrices, such as polypropylene, polylactic acid, (bio-)epoxy resin, bio-phenolic (or tannin) resin, and a few others [12,13]. Standards and guidelines come along with biobased products, such as those dedicated to the determination of the tensile properties of flax fibers [14]. The use of flax fibers as short fibers by injection molding or extrusion results in composites with limited mechanical properties dominated by the properties of the matrix. But the use of long fibers as reinforcement in composite materials may allow us to exploit their properties, and improve their mechanical performances. Most studies on flax biocomposites are focused on the use of long fiber reinforcements in the form of unidirectional (UD) preforms composed of aligned fibers that present better uniaxial mechanical properties in the fiber alignment direction [15–17]. Few studies have investigated the behavior of composite materials reinforced by woven fabrics [16–21]. Indeed, woven fabric manufacturing consists of interlacing a set of warp linear structures with a set of crossing weft linear structures, which can be twisted threads to give sufficient inter-fiber cohesion to the roving. However, with significant twisting, rovings become more compact, which might prevent a good wetting of the fibers during composite manufacturing. For this reason, wrapped rovings could be considered challenging alternatives as they may induce an improvement in the roving weaveability and mechanical properties without any microstructural modification of the fiber [22]. The wrapping process presents a good alternative to improving these mechanical performances with a low environmental impact because no modification is required, neither of the microstructure nor of the chemical composition [23]. Corbin et al. [23] showed that the wrapping process improves the mechanical performance of hemp rovings by 50%. PLA/hemp co-wrapped hybrid yarns were produced by the wrapping process and used for the manufacturing of composite materials [24]. They demonstrated that the tensile and flexural strengths of the composites were improved due to the decrease in porosity resulting from the wrapping process. On the other hand, the mechanical properties of the resulting biocomposites are strongly affected by the fibers surface physico-chemistry. Indeed, the polar components of the surface energy of flax fibers make them difficult to wet with epoxy matrix. It has been proven by Liotier et al. [24], that this difference between fiber surface energy and liquid resin surface tension components leads to micro-void formation at the surface of fibers. The micro-void ratio has a major effect on the mechanical behavior of composites that could outmatch the potential benefits to fiber and yarn mechanical performance [25]. This is why modifying the surface properties of fibers at the scale of yarns and fabrics is of first interest in the manufacturing of performant composites [26,27]. Teraube et al. [28] recently carried out a study that demonstrates that surface modifications of flax fibers can reduce their polarity. This modification allows the treated fibers to become more compatible with polymers with low polar components for the surface tension. A detailed and comprehensive description of the challenges and solutions associated with lignocellulosic fiber-reinforced polymer composites was also reviewed by Ramachadran et al. [29] or Sanjay et al. [6]. The authors point out numerous efficient chemical (pre-) treatments on natural fibers to reduce their hydrophilic nature by eliminating hydroxyl groups. Among them, alkaline pre-treatment was the simplest and most cost-effective, whereas silane, permanganate, benzoyl chloride, acetic acid, and maleic anhydride-grafted polypropylene (MAPP) yielded good results too. This last one is actually a challenging coupling agent, used to strengthen the adhesion between the fibers, usually glass or cellulose fibers, and the polymeric matrix, mainly thermoplastic polyolefin-based resin such as polypropylene (PP). As concerns silane coupling agents, numerous studies demonstrate that they are the most widely used molecules to improve the compatibility and interfacial adhesion between natural fibers and polymer matrices [30–36]. Organosilane coupling agents are generally used for glass fiber sizing [36–39] and more recently for functionalization of lignocellulosic fibers [32,40]. Different lignocellulosic fibers were silanized, including pure cellulose [41], hemp fibers [42,43], cotton fibers [44], flax fibers [42,45,46], ramie fibers [47], sisal fibers [48,49], kenaf fibers [42,50]. Organosilane

chemical structure is designed to form covalent bonds at the fiber-matrix interface, as the silanol group may react with the hydroxyl groups of the lignocellulosic fibers while the organic group (with amino-, vinyl-, and methacryl-functions for example) may react with functional groups of the matrix [23,33]. Hasan et al. [51] reviewed recent progress in the use of organosilanes as coupling agents for lignocellulosic fibers in biocomposites. Other approaches are emerging, including the use of biobased molecules as coupling agents. Acera Fernández et al. [52] used amino acids and polysaccharides as coupling agents to improve the flax fiber/matrix interface in epoxy-based composites. Chitosan has also been used for cotton [53] and flax modification [54]. Laccase has been used in combination with diethylene glycol (DEG) to chemically modify jute fibers, increasing their hydrophobicity and making them suitable for composite reinforcement [55]. In this study, tannins were chosen as bio-based molecules. Tannins are phenolic biopolymers found in most plant species and play an important role in protecting trees from predation and other types of environmental stress. Tannins, which are divided into condensed polymers composed of flavonoid-based subunits and hydrolyzable tannins, which include two subclasses such as gallotanins and ellagitanins [56], have aroused scientific interest due to their phenolic polyaromatic structure. Hydrolyzable tannins are polymers containing a central core of polyalcohol, such as glucose or osidic core, linked partially or entirely to gallic acid (gallotanins) or to hexahydroxydiphenic acid (ellagitanins) via ester connections [56,57]. Condensed tannins are obtained by polymerizing flavanols in the form of oligomeric structures, 3 to 8 flavonoid repeat units are required to form oligomers. Each flavonoid is composed of two phenolic rings (A and B) with different reactivities [58]. Condensed and hydrolyzable tannins can be used as charring agents in intumescent flame retardant systems when functionalized due to their highly carbonated aromatic structure [59,60]. However, up to our knowledge, condensed tannins have not yet been used as coupling agents to improve the flax fiber-matrix interface in biocomposites. Condensed tannins can be used as a coupling agent in composite materials because their high molecular weights and strong hydrogen bonding can improve the mechanical properties and interfacial adhesion of the composite. Bayart et al. [61] have, for example, shown that quebracho tannins have good compatibility with flax fibers, making them easy to incorporate into PLA (polylactic acid) polymers. Additionally, tannins can also act as a natural cross-linking agent and improve the thermal stability of composite materials. This makes condensed tannins a potential alternative to traditional coupling agents in sustainable composite materials. In addition, condensed tannins represent more than 90% of the world's production of commercial tannins and are considered economically important. Condensed quebracho tannins were chosen in this study because of their high tannin content, which makes them an effective flame retardant compared to other tannins [62]. The choice of condensed quebracho tannins was also motivated by a preliminary study in which a large variety of hydrolyzable tannins, such as tannic acid, oak tannin, and chestnut tannin, and condensed tannins, such as quebracho tannin, were compared through an evaluation of their ability to act as flame retardants. From these analyses, it has been concluded that condensed quebracho tannin has the greatest potential as a flame retardant because of its high char content, which acts as a protective layer.

In the present study, a chemical functionalization of wrapped flax rovings with a condensed quebracho tannin was investigated to act as a biobased coupling agent for further epoxy/flax fabric biocomposites applications. The chemical functionalization of wrapped flax rovings was performed using an innovative lab-scale impregnation line. The efficiency of the chemical grafting was evaluated (FT-IR and SEM-EDX experiments), as well as the weaving ability of the treated rovings by manufacturing plain and satin flax fabrics using a manual shuttle loom. A comparison with a non-bio-based molecule, i.e., a 3-aminopropyltriethoxysilane, was carried out. The influence of the tannin and silane concentrations (1% and 5% in weight) was also studied. The influence of chemical treatment on the mechanical properties either of the rovings or of the fabrics was reported, along with the effect of the weaving steps on the mechanical characteristics of wrapped flax rovings.

2. Materials and Methods

2.1. Materials

2.1.1. Wrapped Flax Rovings

A wrapped flax roving (linear density of 500 tex) with a flax core wrapped by a cotton yarn with no additional treatment was provided by the company "Terre de Lin" (Saint-Pierre-le-Viger, France). The rovings are composed of a parallel arrangement of flax fibers aligned along the rovings' longitudinal axis that have undergone several combing and regularization stages, meaning that they do not contain fibers oriented in the opposite direction and spun cotton yarns as wrapping yarns, as shown in Figure 1.
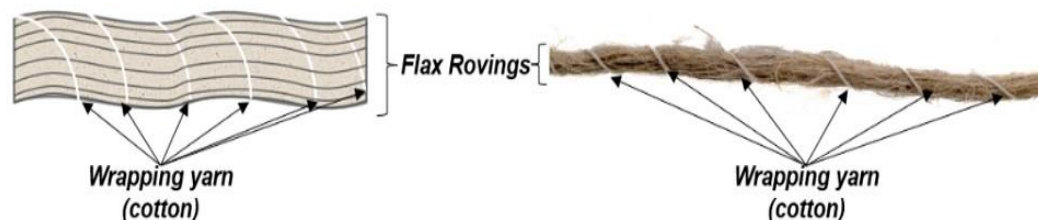
Figure 1. Structure of a cotton-wrapped flax roving as used in this study.

2.1.2. Molecules for Surface Treatment of Wrapped Flax Rovings

Acetic acid (96%), sodium hydroxide (40 g/L) and 3-aminopropyltriethoxysilane (APTES) (Figure 2a) were purchased from Sigma Aldrich. Fintan Q® condensed tannins extracted from quebracho wood named Q (Figure 2b) were purchased from Silva Chimica (San Michele Mondovi, Italy). Demineralized water was used for the preparation of organosilane and tannin solutions.

(a)   **(b)**
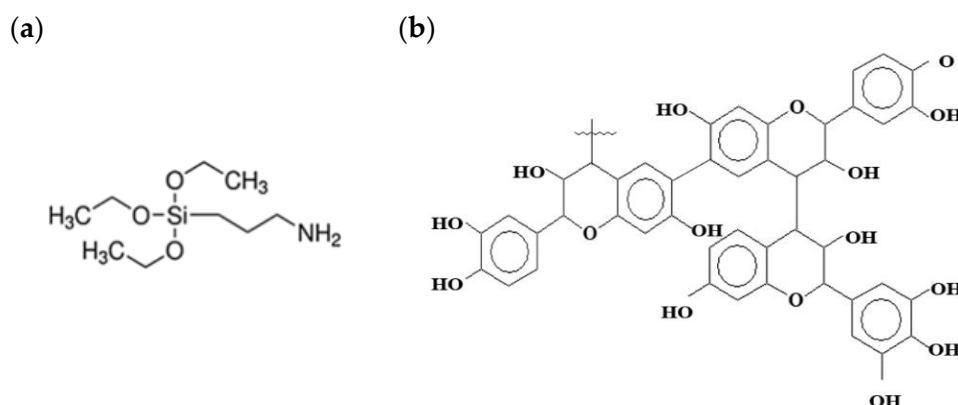
Figure 2. Chemical composition of (**a**) 3-aminopropyltriethoxysilane (APTES), (**b**) Quebracho tannin (Q).

2.2. Processing

2.2.1. Preparation of the Solutions for Surface Treatment

APTES solutions were first hydrolyzed in a 60/40 wt.% water/ethanol solution at two concentrations (1 and 5 wt.%). pH was adjusted to 5 using acetic acid. The solution was stirred for 1 h at room temperature. The quebracho tannin powder was diluted in water at a concentration of 5 wt.% and stirred for 40 min. The pH of the solution is around 5. 1 wt.% sodium hydroxide was added and stirred until complete homogenization. The pH of the solution is around 11. The nomenclature used for flax rovings in this study is presented in Table 1.

Table 1. Description of flax rovings in this study.

Abbreviation	Description
UR	Untreated rovings
TRS1	Treated rovings with 1 wt.% APTES solution
TRS5	Treated rovings with 5 wt.% APTES solution
TRQ5	Treated rovings with 5 wt.% quebracho tannins
TRQ5N1	Treated rovings with 5 wt.% quebracho tannins + 1 wt.% NaOH

2.2.2. Impregnation Line

The impregnation line (Figure 3) is an experimental pilot prototype allowing the continuous impregnation of linear structures such as yarns and rovings. It is composed of six main sections: the unwinding of the roving bobbin, where the unwinding tension is controlled by a pressure sensor, then the mounting, followed by the impregnation bath and the infrared oven before the bobbin winder. Three types of configurations were available on the used lab-scale impregnation line, called the W, V, and J configurations (Figure 4), corresponding to how the roving is threaded onto the impregnation line. The W configuration was chosen as it allows the rovings to spend more time in the chemical solution bath and drying than the other configurations. Throughout the impregnation process, the roving is controlled by guide rollers. At the exit of the bath, the roving goes to an infrared oven set at 80 °C with three passages to evaporate water and induce the grafting reactions of the molecules onto the roving. At the end of the line, the treated and dry roving is wound onto a bobbin, which controls the winding speed of the entire line.
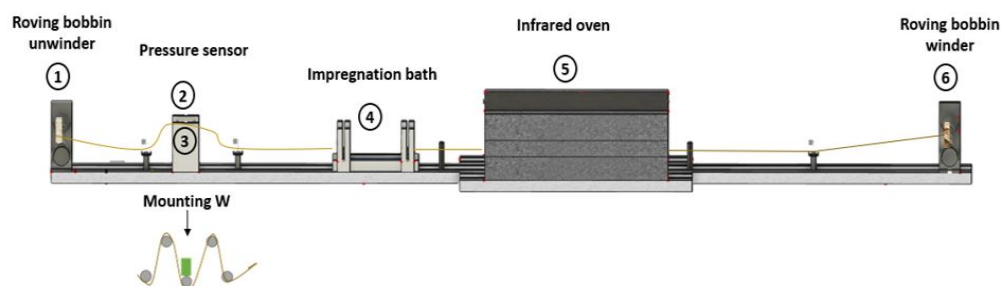
Figure 3. Impregnation line used for wrapped flax roving grafting: roving bobbin ①, pressure sensor ②, mounting ③, impregnation bath ④, infrared oven ⑤, bobbin winder ⑥.

Figure 4. The different types of assembly possible on the impregnation line.

2.2.3. Fabric Manufacturing

Weaving is a fabric production process that consists of interlacing perpendicularly two sets of yarns. The warp runs longitudinally in the direction of the loom, while the weft runs perpendicularly. A manual shuttle loom, called weavebird, from Leclerc Company (Canada) was used at ENIT (Tarbes, France) was used (Figure 5). The technical parameters of the desired fabric, such as the width of the fabric, the weaving pattern, and the density of the fabric, were previously determined. Several operating steps are necessary to weave. The first step is the preparation for warping, which consists of preparing bobbins of suitable characteristics containing equal lengths of yarn and mounting them on the creel for the warping operation. The second step is the warping itself, which consists of unwinding the warp yarn spools. These warp threads are inserted in a third step, one by one, into the heddles of the frames at the stretching stage and then into the reed at the stitching stage, and the threads are then put under tension. Weave tracing is performed by Fiberworks Sliver

4242® software, and the weaving can start. The frame movement leads to the formation of the shed, which is the result of the separation of the warp yarns into two layers: upper (taken) and lower (left). When the weft is inserted, a shed occurs between the warp threads that are caught. Once the weft is inserted and pressed against the fabric, the lowered warp threads rise while the raised ones fall, creating a shed. Two types of weaves were manufactured (Table 2, a plain (P) and satin (S) of 5-harness satin. The wrapped rovings were used in both warp and weft directions. Several fabrics were produced for each type of weave (Table 3), UP and US with untreated wrapped rovings, TPS1 and TSS1 with 1 wt.% APTES treated wrapped rovings, TPS5 and TSS5 with 5 wt.% APTES treated wrapped rovings, TPQ5 and TSQ5 with 5 wt.% condensed tannins treated wrapped rovings, TPQ5N1 and TPQ5N1 with 5 wt.% condensed tannins, and 1 wt.% NaOH treated wrapped rovings. The warp density is 5 in-cm, and the weft density is 5 rovings/cm for all the fabrics.
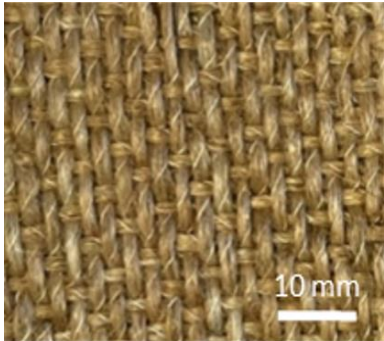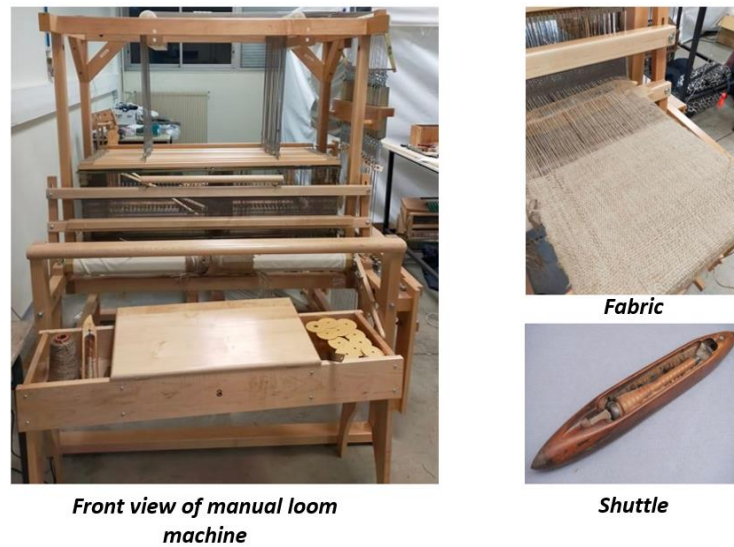

Front view of manual loom machine

Fabric

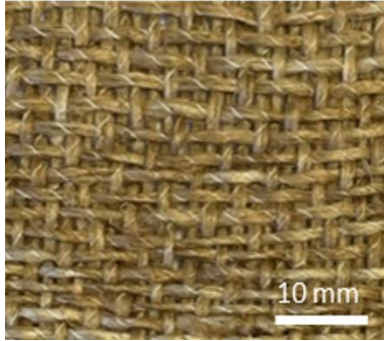*Shuttle*

Figure 5. Shuttle manual loom machine.

Table 2. Weave pattern of the resulting flax is woven on plain and satin fabrics.

Plain Woven	Satin Woven
Ratio of 2	Ratio of 5
1 wrap thread × 1 weft thread	5 wrap threads × 5 weft threads
Offset 1	Offset 2

Table 3. Nomenclature used for the different fabrics of this study and photographs of the resulting flax-woven plain and satin fabrics.

Abbreviation	Description	Abbreviation	Description
UP	Untreated plain	US	Untreated satin
TPS1	Treated plain with 1 wt.% APTES	TSS1	Treated satin with 1 wt.% APTES
TPS5	Treated plain with 5 wt.% APTES	TSS5	Treated satin with 5 wt.% APTES
TPQ5	Treated plain with 1 wt.% Q	TSQ5	Treated satin with 1 wt.% Q

Table 3. *Cont.*

Abbreviation	Description	Abbreviation	Description
TP5N1	Treated plain with 5 wt.% Q + 1 wt.% NaOH	TSQ5N1	Treated satin with 5 wt.% Q + 1 wt.% NaOH

2.3. Characterization Methods

2.3.1. Fourier Transform InfraRed Spectroscopy (FT-IR)

Spectroscopic analyses were performed using a Bruker Vertex 90 FT-IR spectrophotometer in the spectral range of 4000–400 cm^{-1} with a resolution of 4 cm^{-1} and 32 scans using the standard ATR device.

2.3.2. Scanning Electron Microscopy (SEM-EDX)

Scanning electron microscopy (SEM) (FEI QUANTA 200, acceleration voltage 12.5 kV) was used to observe the microstructure of the samples. Samples were prepared by depositing a layer of carbon before analysis. EDX analyses (Oxford Instrument 80 mm^2 XMAX detector) have been performed to determine the elemental chemical composition and to develop a map of the distribution of silica elements. A preparation step is necessary, which consists of dipping vertically in a transparent epoxy resin pad of ESCIL Geofix® type (Chassieu, France) with a curing time of 24 h at room temperature.

2.3.3. Mechanical Characterizations

Mechanical Properties of Rovings

Tensile tests were performed on untreated and treated wrapped rovings using a Zwick/Roell Z010 (Zwick/Roell, Ulm, Germany) tensile device equipped with a 1 kN load cell, according to the ASTM C1557 standard [63]. The tensile properties of linear structures depend on the length of the sample between jaws due to the different deformation and breaking mechanisms involved in a tensile test (fiber breakage, slippage, and disengagement of fibers). To study the effect of the gauge length on the tensile properties, three different gauge lengths were tested, namely 25 mm, 50 mm, and 100 mm. The choice of gauge lengths was based on increasing the distance between the gauges to enclose the length distribution of the elementary flax fibers in the rovings and to have some measuring points well above the maximum length of the elementary fibers as well as the length of the fibers. Tests were carried out in displacement control at a crosshead speed of 2 mm/min with a preload of 1 N. For each gauge length and roving treatment, thirty rovings were tested. These tensile tests were carried out at room temperature. A preliminary drying was carried out for 24 h at 80 °C to remove moisture from the fibers. This is an important step in ensuring the reliability and consistency of the data obtained while guaranteeing that all samples have the same moisture content and preserving the quality of the samples intended for testing. The tenacity of a roving is defined as the force (cN) per the linear density (tex). In the case of textile yarns, the mechanical tensile properties per unit of linear mass and not per unit of cross-sectional area were defined considering that textile yarns are usually compressible. However, since the fineness of a yarn depends on the ratio of its

weight to its length, and since both length and weight can always be measured accurately, the fineness of a yarn is expressed as an indication of the relative weight to the length. The unit of measurement is, therefore, weight in grams per kilometer. This quantity is called "linear density" and is expressed in Tex. The linear density was evaluated after each chemical treatment for 10 rovings according to the NF G07-316 standard [64].

Mechanical Properties of Fabrics

Mechanical properties were also performed on untreated and treated flax fabrics according to ASTM D5035. Tensile tests were performed at room temperature by using a Zwick/Roell Z010 (Zwick/Roell, Ulm, Germany) device equipped with a 1 kN load cell. Tests were performed with an extension rate of 200 mm/min, a gauge length of 75 mm, a specimen width of 25 mm, and a preload of 5 N. A preliminary drying was carried out for 24 h at 80 °C to remove moisture from the fabrics. A mean value for six samples per treatment and per direction is determined. The thickness and areal density are measured according to the NF EN ISO 5084 standard [65], and the NF EN 12127 standard [66], respectively. For each sample, the number of yarns was counted to determine the specific load per roving (N/tex) to consider roving fineness and the fabric frame.

3. Results and Discussion

3.1. Evaluation of the Molecule Grafting Efficiency on Wrapped Flax Rovings

3.1.1. Physico-Chemical Characterization

APTES Treatments

FTIR analysis was carried out on untreated and treated-wrapped flax rovings in order to determine the presence of grafted molecules on the flax fiber surface (Figure 6a). IR spectra give evidence of the characteristic peaks of flax fibers. Peaks located at 3340 and 2900 cm^{-1} correspond to stretching vibrations of hydroxyl and alkane groups in polysaccharides. The peak located at 1731 cm^{-1} is related to the C=O ester band in hemicellulose. The peak at 1630 cm^{-1} is attributed to water within cellulose [67,68]. The peak located at 1507 cm^{-1} corresponds to C=C symmetrical stretching of the aromatic ring of the lignin. The absorption bands at 1422, 1373, 1337, 1203 and 896 cm^{-1} may belong to stretching and bending vibrations of -CH2 and -CH, -OH, and C-O bonds in cellulose, respectively. The C-O-C glycosidic ether band is located at 1157 cm^{-1}. Due to APTES treatment, the presence of a new peak located at 1564 cm^{-1}, corresponding to the bending vibration of the amino group (-NH2) of silane [24] is observed. This can be explained by a reaction occurring between APTES silanol functions and the cellulose hydroxyl groups of flax fibers [45,69,70] creating a covalent C-O-Si bond. For a semi-quantitative analysis, all spectra were normalized considering the band located at 1203 cm^{-1} that is related to the OH group in-plane bending vibration of cellulose [71]. Thus, the ratio between bands at 1564 cm^{-1} and 1203 cm^{-1} was determined and is presented in Figure 6b. The presence of amino groups on the flax fiber surface after APTES treatment was confirmed by an increase in this ratio with the silane concentration [52,56,72].

In addition, SEM-EDX analyses were carried out (Figure 7) to localize Si atoms (from silane) onto the fibers. Results showed the presence of Si on the surface and in the core of the filaments. Silane may therefore penetrate the pores, voids, and interstices and develop a mechanically interlocked coating on the surface of lignocellulosic fibers. Müssig et al. [73] found a relatively high porosity (10%) content on the surface of flax fibers, which allows the molecules to migrate into the fiber within their porous structure. The concentration of APTES (1 and 5 wt.% for TRS1 and TRS5 flax, respectively) had a significant impact. Indeed, the ratio between the bands at 1564 cm^{-1} and 1203 cm^{-1} was four times higher for TRS5 than for TRS1.
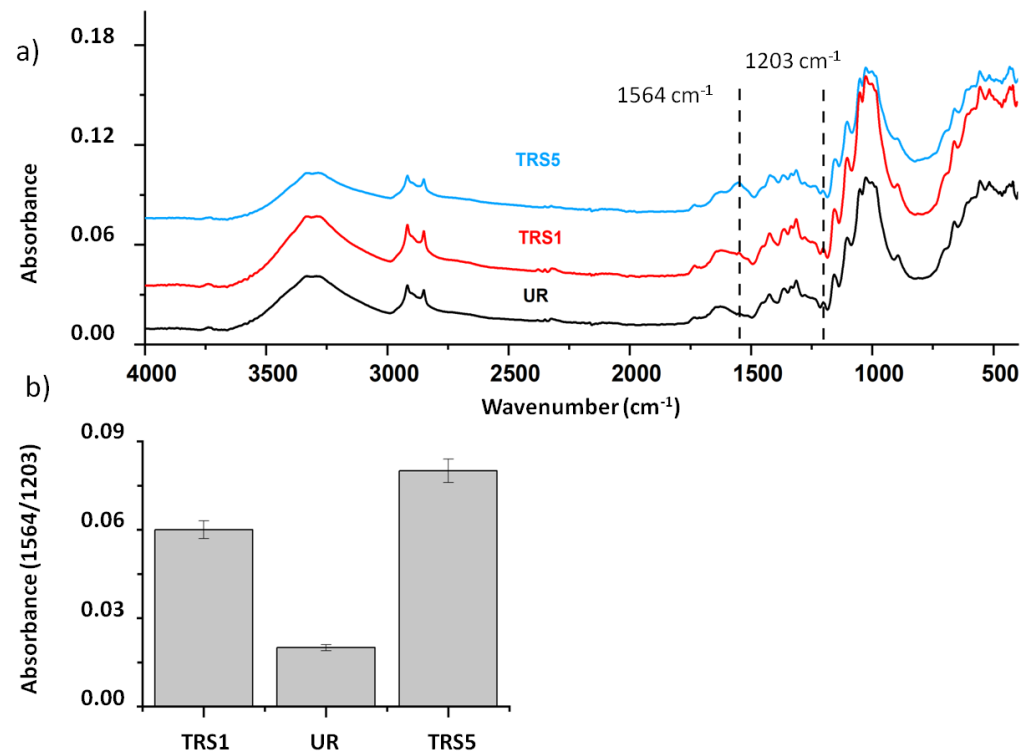
Figure 6. (**a**) FTIR-ATR spectrum of rovings treated with APTES at different concentrations, (**b**) Ratio between the intensity of the FT-IR bonds located around 1564 cm^{-1} and 1203 cm^{-1} of untreated and APTES (1 and 5 wt.%) treated wrapped flax rovings.
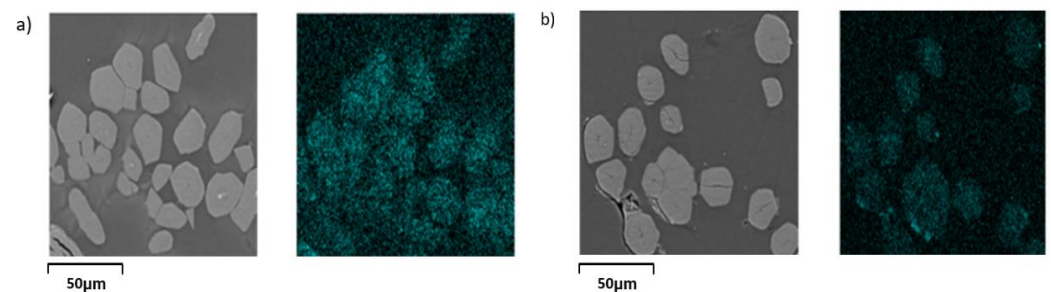

Figure 7. SEM-EDX cartography of silica localization onto APTES 1 wt.% (**a**) and 5 wt.% (**b**) treated wrapped flax rovings.

Assumptions could be made that this silane grafting onto flax fibers may optimize the quality of adhesion at the interface between the silane-modified flax fibers, and the epoxy resin through covalent bonds between the amine groups from aminosilane and the epoxy functions from epoxy resin [74]. The proposed scheme of reaction mechanims between flax fibers treated with silane and epoxy gives an idea of the modified flax interphase with silane/epoxy (Figure 8).

Quebracho Tannins Treatments

The structure of polyphenols contains both hydroxyl groups and aromatic rings, allowing interactions with cellulose by physical adsorption through non-covalent interactions such as hydrogen bonds and hydrophobic forces, as demonstrated by Shan et al. [75]. For this reason, it can be assumed that the OH functions of the tannins can interact through bonds with the OH, COOH, and COH functions of the cellulose, hemicellulose, pectins, waxes, and lignin components of flax fibers. Esterification reactions can be involved between acid groups of pectins or waxes of flax fibers and hydroxyl groups of tannins, as shown in Figure 9, leading to the formation of O-C=O bonds. Etherification reactions can

also be involved between OH functional groups of tannins and OH groups from cellulose, hemicellulose, pectins, waxes, and lignins of flax fibers, as shown in Figure 9, leading to the formation of C-O-C bonds. It is also possible to form hemiacetals (CH-OH) from the interaction between the OH functions of tannins and aldehyde groups in waxes (Figure 9). To provide evidence of these interactions, an IR analysis was performed. Figure 10a shows the IR spectra of raw quebracho tannins, and of untreated and treated flax rovings with these tannins. The analysis was focused on peaks located at 1610 cm^{-1} and 1510 cm^{-1} both related to C=C stretching of the aromatic ring and on the peak located at 1420 cm^{-1} attributed to C-O and O-H groups in tannins. All the spectra were normalized considering the band located at 1203 cm^{-1} related to OH in-plane bending vibrations of cellulose that is not influenced by all chemical treatments [69]. Thus, the absorbance ratios between bands located at 1610 cm^{-1}, 1510 cm^{-1}, 1420 cm^{-1} and the band at 1203 cm^{-1} were calculated for each treatment, and the results are presented in Figure 10b. It can be observed that there is an increase in all ratios when comparing TRQ5 (5 wt.% of tannins) to UR (untreated). This increase indicates the presence of tannins on the surface of the flax bundles. Moreover, Nam et al. [76] have shown that the addition of a low concentration of NaOH increased the adsorption of tannic acid on non-woven cotton fabrics. The visual aspect of flax rovings as a function of the addition of NaOH changed, and it has been observed that its color is browner than the one treated only with tannins. In agreement with the literature, Figure 10a shows that the spectrum of TRQ5N1 has peaks with higher intensities at 1610 cm^{-1}, 1510 cm^{-1}, 1410 cm^{-1} than TRQ5. However, Friedman et al. [77] investigated the effect of pH on the stability of plant phenolic compounds, and showed that condensed tannins are more stable with increased pH. Intensive research devoted to the development of natural dyes from various bio-based products [78] showed that the dyeing of cellulosic fibers requires a high pH in order to promote the rise of the dye in the fiber, as a cellulosate anion can be involved, inducing the creation of strong covalent bonds.
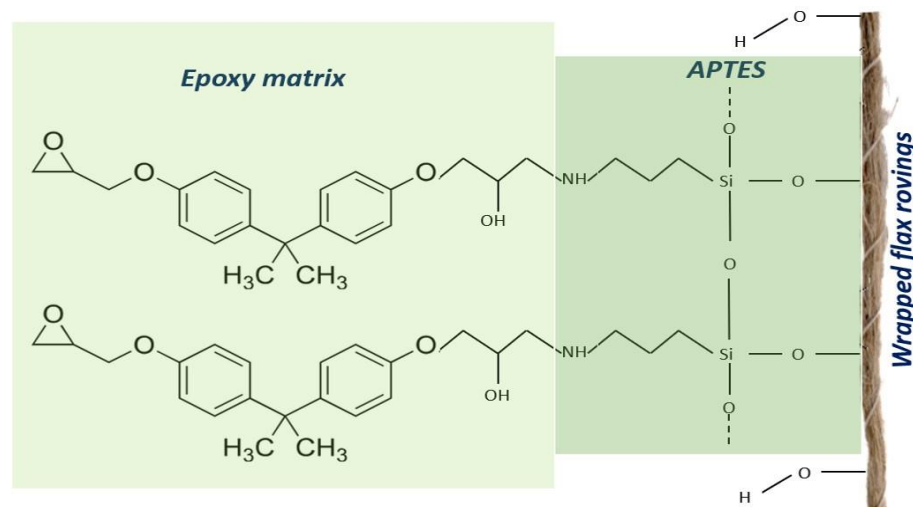

Figure 8. Assumptions concerning the interfacial reactions between silane-treated flax-wrapped rovings and epoxy matrix.

Grafting quebracho tannins onto flax surfaces offers the possibility of optimizing the quality of adhesion at the interface between flax and epoxy by inducing chemical changes through the incorporation of tannins. Assumptions could be made that this tannin grafting onto flax fibers may optimize the quality of adhesion at the interface between the flax fibers and the epoxy resin through covalent bonds between the hydroxyl groups from polyphenol and the oxirane functions from epoxy resin, creating a new ether bond. This epoxidation reaction is commonly used in the manufacture of fiber-reinforced polymer composites, corrosion-resistant coatings, adhesives, and other chemicals and materials. It creates strong bonds between polyphenols and epoxies, improving the mechanical and

chemical properties of the resulting materials [79]. The proposed schematic of the reaction mechanism between flax-grafted tannins and the epoxy matrix provides an overview of the resulting interphase (Figure 11).
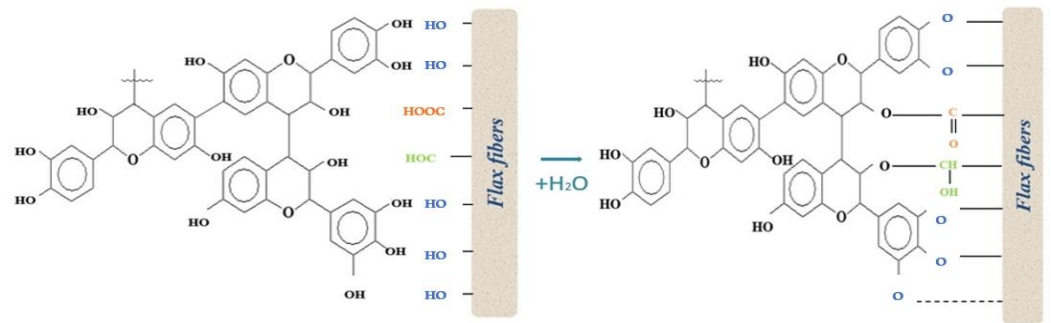
Figure 9. Potential grafting reactions of tannins on flax fibers surface (orange = esterification; green = hemiacetalization; blue = etherification).
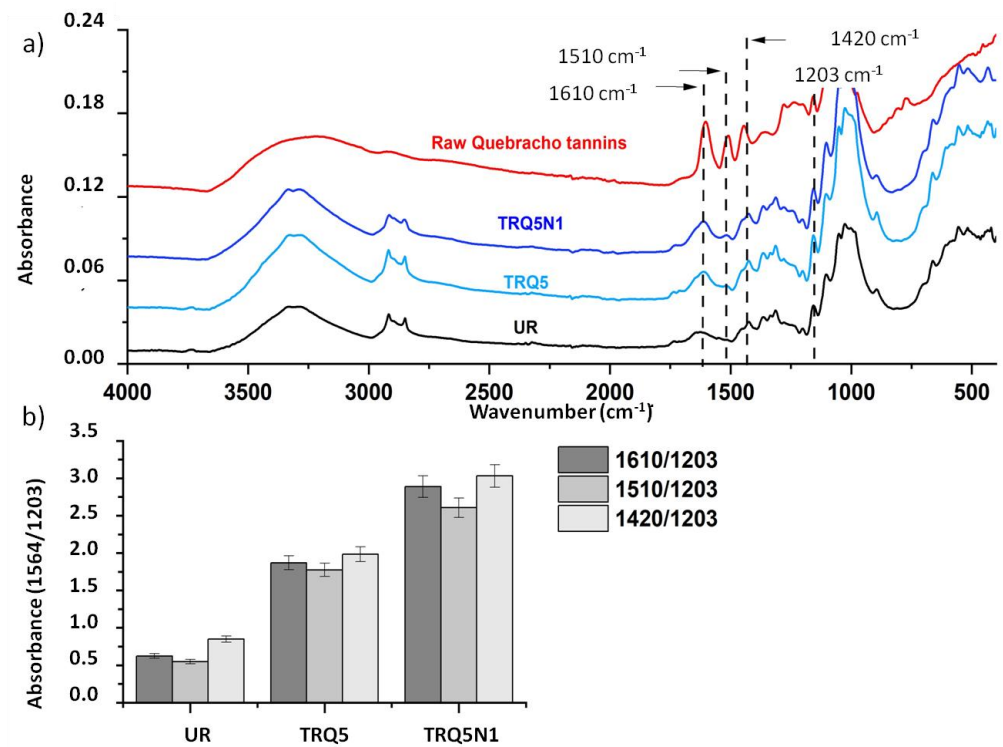

Figure 10. (**a**) FTIR-ATR spectrum of raw Q tannins compared to untreated rovings (UR) and rovings treated with 5 wt.% Q (TRQ5) or with 5 wt.% Q and 1 wt.% NaOH (TRQ5N1), (**b**) Ratio between the intensity of FT-IR bonds located around 1610, 1510 and 1420 cm^{-1} and the intensity of the bonds located at 1203 cm^{-1} considered as a reference of UR, TRQ5 and TRQ5N1.

3.2. Influence of the Surface Treatments on the Tensile Properties of Wrapped Flax Rovings

3.2.1. Effect of the Gauge Length

The evolution of the tensile properties of the untreated and treated rovings as a function of the gauge length is presented in Figure 12. The boxplots represent the median value (with the first and third quartiles) of the tenacity obtained for each gauge length and for each chemical treatment. The error bars represent the maximum and minimum values obtained for the 30 tests performed, represented by square dots, and the dispersion is plotted as curves beside the experimental values. As expected, the gauge length has a significant influence on rovings' tenacity. The maximum force at breakage tends to decrease with increasing gauge length. The same observation has been noted for elementary flax fibers and for flax fiber bundles in the literature [34,79].
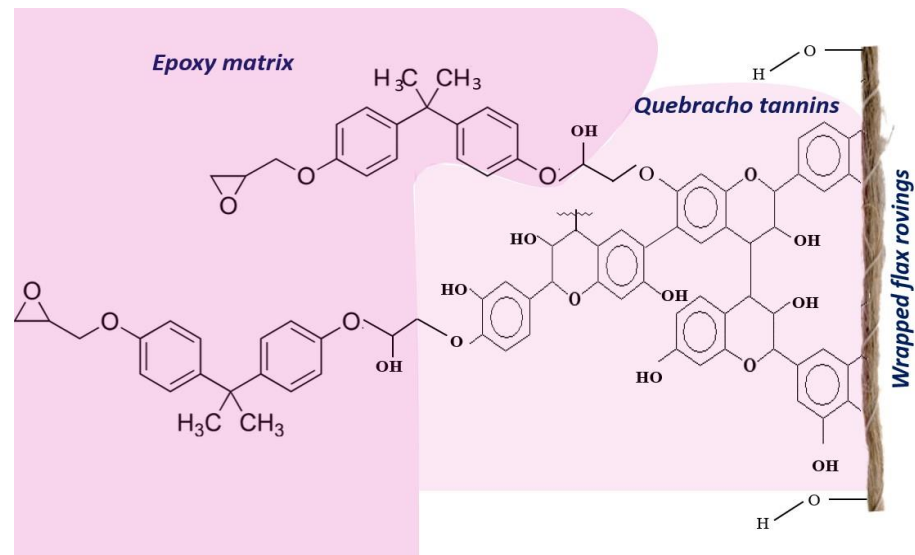
Figure 11. Assumptions concerning the interfacial reactions between quebracho tannin-treated flax-wrapped rovings and epoxy matrix.
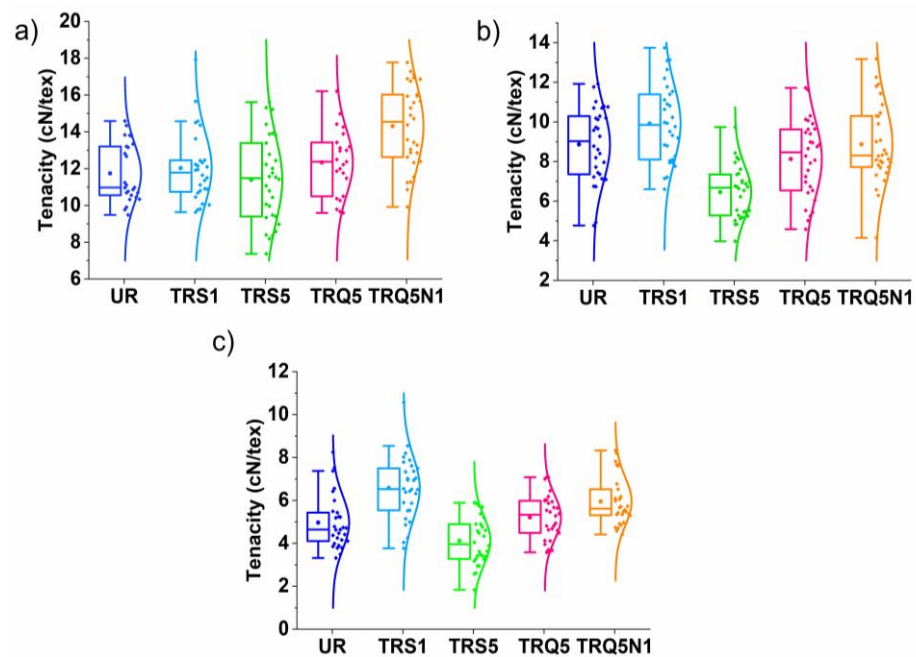
Figure 12. Tensile behavior of untreated and treated wrapped rovings at different gauge lengths: (**a**) 25 mm, (**b**) 50 mm, and (**c**) 100 mm (circles = median; diamonds = values).

In the case of an elementary fiber, the tensile test is usually performed with a gauge length smaller than the fiber length. In the case of fiber bundles, if the gauge length is small, all the elementary fibers will be tested. Conversely, if the gauge length is too high, it is possible that some fibers, which are shorter than others, will not be tested, which would influence the measured properties. This phenomenon is related to a poor interface between the elementary fibers within the bundle, according to the literature [80,81]. The length distribution of the elementary fibers also varies according to the flax variety, the retting conditions, and the fiber extraction processes such as scutching and hackling. Müssig [73] reported a length of the elementary fibers of about 33 mm that is higher than the gauge length of 25 mm and lower than the gauge lengths of 50 mm and 100 mm. The presence of surface defects can also influence the mechanical results of tensile loading, especially the tensile strength. Baley and Bourmaud 8 and Bos and Donald [82] reported that, in a tensile

test, failure occurs mostly in the vicinity of a defect. However, when considering that there are surface defects in elementary fibers, the presence of defects can thus be expected in the whole bundle of fibers and therefore in the rovings. Therefore, when the gauge length increases, the number of defects inducing fiber breakage may also increase. For a better understanding, the location of fiber breakings according to gauge length is highlighted in Figure 13.
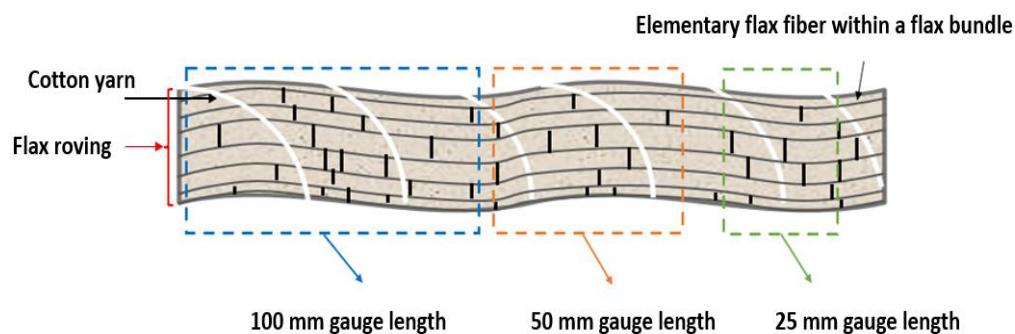
Figure 13. Illustration of the elementary fibers, and bundle fibers in wrapped flax roving.

3.2.2. Effect of the Chemical Treatment

As shown in Figure 14 whatever the gauge length, in the case of rovings treated with 1 wt.% APTES solution (TRS1), an increase of 3% for 25 mm, 8% for 50 mm, and 39% for 100 mm in the breaking tenacity can be observed after treatment compared to untreated rovings, while for rovings treated with 5 wt.% APTES (TRS5), a decrease of 3% for 25 mm and 50 mm and of 9% for 100 mm was highlighted.

Based on all these results, it can be assumed that a polysiloxane monolayer network is created on the fiber surface in the case of a 1 wt.% APTES treatment, while a 5 wt.% APTES treatment can produce a multilayer polysiloxane network. In this case, Georgiopoulos et al. [43] performed a comprehensive study with different concentrations of APTES. The authors found that an optimal silane concentration of 2 wt.% may provide better mechanical properties to the PLA/unidirectional flax bio-composite, probably due to better penetration of the silane onto the fibers, compared to higher amounts (5 wt.% silane content). Le Moigne et al. [45] optimized the silane treatment conditions (silane concentration, soaking duration, and temperature) in the case of flax fibers and studied their influence both on the fiber wettability and the mechanical properties of the PLA/flax biocomposites. These authors showed that a good balance between the chemical coupling reaction between the hydroxyl and carboxyl end groups of PLA and the hydroxyl and acidic groups at the flax fiber surface, as well as mechanical interlocking mechanisms (surface roughness), should be provided. Sepe et al. [83] studied the effect of silane treatments with different concentrations on the surface of hemp fibers and improved their interfacial interactions with an epoxy resin. It was found that a concentration of 1 wt.% of silane is the optimum condition as regards the mechanical properties of epoxy/hemp fabric biocomposite.

In the case of bio-based treatments, an increase in the breaking tenacity is observed for TRQ5 (4.5% for 25 mm and 12.5% for 50 mm) and TRQ5N1 (22% for 25 mm and 28% for 100 mm) for all the gauge lengths. Literature gives evidence that a low concentration of NaOH enhances the adsorption of tannins onto cotton fabrics. Thus, pH has an important effect on the result of chemical treatment of lignocellulosic fibers [84]. NaOH potentially eliminates some extractables and thus favors the absorption kinetics of tannin in the flax fiber. Research has demonstrated that alkaline treatments increase surface roughness, thus revealing more cellulose and enhancing the number of accessible reactive sites. For a better understanding of the impact of chemical treatments on the physico-chemical properties of flax fibers, it is important to make measurements of surface properties. Acera Fernández et al. [85] analyzed the role of flax cell wall components on the physico-chemical properties of flax fabrics. They demonstrated that using NaOH resulted in high yields of

extraction for non-cellulosic components, leading to an increased hydrophilicity of flax fabrics, and thus, a decrease in the initial contact angle and an increase in the rate of water absorption. However, many studies have highlighted the use of NaOH as a pre-treatment, which (i) removes impurities from the surface of the fiber, and (ii) improves the chemical reactivity of the fibers by opening the cellulose structures, allowing easier penetration of chemical agents for further processing. Tran et al. [86] showed that the mechanical properties of einkorn wheat husk-reinforced PLA biocomposites can be improved by the combination of alkaline and silane surface treatments. In this case, the cleaning step by NaOH allows activating hydroxyl groups on the surface of the husk and makes them more reactive towards silane compared to the hydroxyl groups present on the surface of the untreated beads.
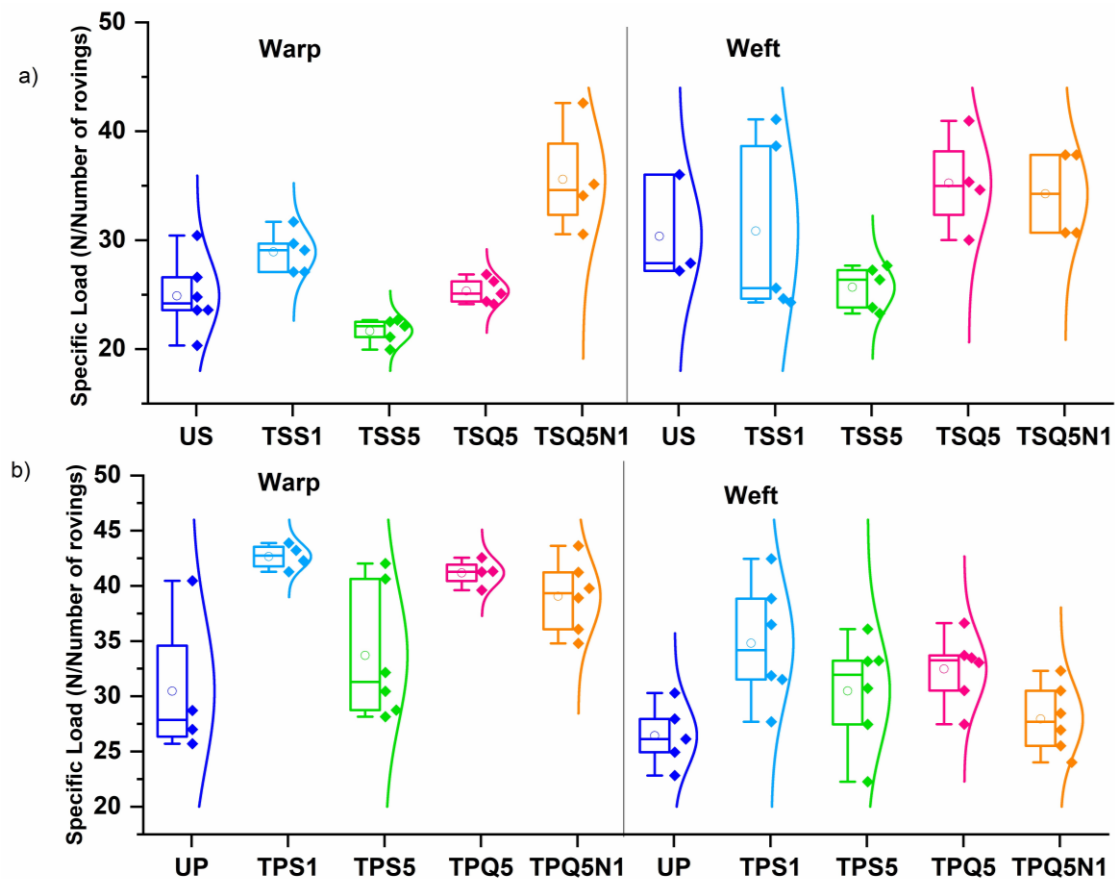
Figure 14. Tensile behavior of fabrics in the warp and weft directions of untreated and treated wrapped flax rovings: (**a**) Plain fabrics and (**b**) Satin fabrics (circles = median; diamonds = values).
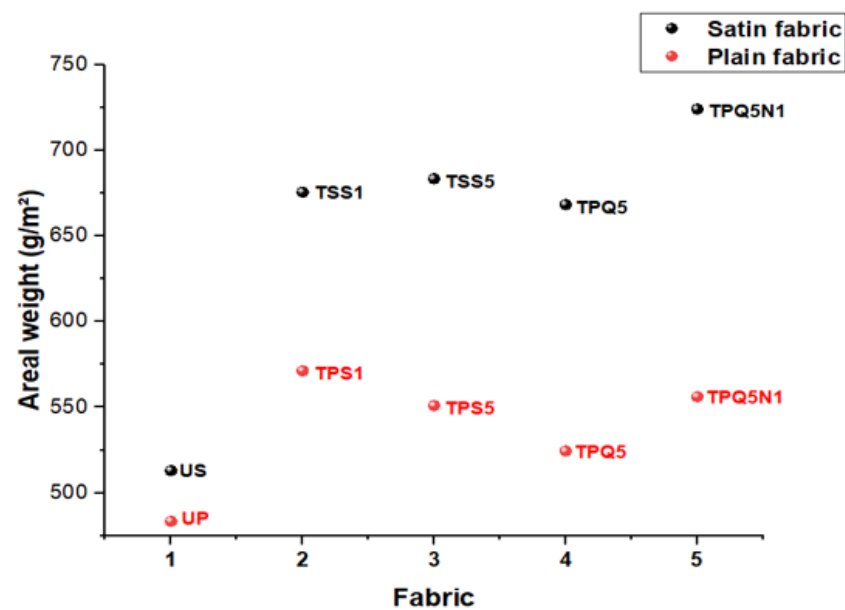
3.3. Evaluation of the Chemical Functionalization of Wrapped Flax Rovings on the Properties of Developed Fabrics

3.3.1. Determination of the Characteristics of Manufactured Fabrics

Woven fabric properties made from untreated and treated wrapped rovings are presented in Table 4 and Figure 15. The areal weight (g/m^2) is defined according to the standard NF EN12127 [66] and the thickness according to the standard NF EN ISO 5084 [65]. Both fabrics, plain and satin, have 5 rovings/cm for warp and weft densities. A higher areal weight was observed for fabrics based on chemically treated wrapped rovings compared to fabrics based on untreated wrapped rovings. Figure 15 shows that the areal weight of the satin fabrics is higher than that of the plain fabrics. The thicknesses of plain fabrics are lower than the thicknesses of satin fabrics. However, all treated fabrics (plain or satin) have a higher thickness than the untreated fabrics.

Table 4. Properties of woven flax fabrics.

| Plain Fabric	Thickness (mm)	Areal Weight (g/m^2)
UP	0.9	484 ± 7
TPS1	1.2	571 ± 6
TPS5	1.2	571 ± 6
TPQ5	1	525 ± 5
TPQ5N1	1	556 ± 13
Satin Fabric	**Thickness (mm)**	**Areal Weight (g/m^2)**
US	1.7	513 ± 31
TSS1	2	676 ± 24
TSS5	2	683 ± 38
TSQ5	1.8	668 ± 38
TSQ5N1	1.8	724 ± 30

Figure 15. Areal weight of untreated and treated flax fabrics.

3.3.2. Influence of Chemical Functionalization of Wrapped Flax Rovings on the Tensile Properties of Fabrics

The tensile behavior of all fabrics (satin and plain) in both directions (weft and warp) (expressed in force at breakage (N) per number of rovings in the samples) as a function of the surface treatment is presented in Figure 14. The boxplots represent the median value (with the first and third quartiles) of the specific load for each chemical treatment. The error bars represent the maximum and minimum experimental values represented by square dots, and the dispersion is plotted as curves beside them. It allows for highlighting the effects of both the roving and fabric density. During the tensile test, the fracture occurred in the middle of the sample in all cases. For satin fabrics, it can be observed that the specific load is higher (+33%) in the weft direction than the warp direction for the untreated satin (US). This can be analyzed regarding the geometry of the satin fabric (satin of weft effect). Therefore, it is formed by floating weft rovings over four rovings before moving to the next weft rovings. Moreover, satin fabrics are generally unbalanced and have less interlacing per unit area than plain weave. The elongation at break is 1.5 times higher in the weft direction than in the warp direction. The same change in the specific load and the elongation at break was observed for fabrics made from chemically treated wrapped rovings. Plain is the simplest woven fabric structure. It is formed by the alternating rise and fall of a warp roving through a weft roving. For the untreated plain fabric, the tensile behavior is the

same in both directions, related to identical linear density and number per unit for warp and weft rovings. It is a balanced fabric compared to satin fabric. The elongation at break of the untreated plain fabric (UP) is three times higher in the warp direction than in the weft direction (Figure 16). Moreover, for all plain fabrics made with chemically treated rovings, an increase in the specific load was observed in both directions, but it was better in the warp direction than in the weft direction. The tensile behavior in the warp direction increases by 60%, 26%, 55%, and 44%, and in the weft direction by 35%, 15%, 23%, and 8% for TPS1, TPS5, TPQ5, and TPQ5N1, respectively. This unbalanced property may be due to the elongation effect, which is more important in the warp direction than in the weft direction for the fabric based on chemically treated wrapped rovings. Moreover, high tension is applied to the warp yarn in the weaving processes. To conclude, whatever the pattern weave (satin or plain), and the chemical treatment nature, an improvement in the mechanical behavior of the woven fabrics was observed. A different behavior has been reported for satin fabrics in comparison to plain fabrics. Thus, during the manufacture of the fabric, the weaveability of all treated and untreated rovings was evaluated during the weaving process, and no roving breakage has been reported.
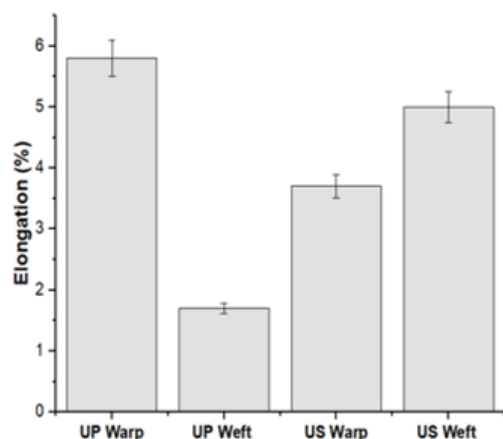

Figure 16. Elongation at break of untreated fabrics (UP = Plain, US = Satin) in the warp and weft directions.

3.4. Evaluation of the Effect of Weaving Process on the Mechanical Properties of Wrapped Flax Rovings

During the weaving process, the rovings have been subjected to cyclic mechanical stresses, which may impact the rovings' mechanical properties. The effect of the weaving process on twisted flax rovings has been studied by Corbin et al. [87]. These authors demonstrated that the improvement in mechanical properties can be attributed to the increase in torsion following the weaving process. Omrani et al. [88] have studied the weaving process's impact on twisted flax yarns, twisted tow flax yarns, and roving yarns. The authors observed degradation during the weaving, and the twist effect can help reduce this degradation. Therefore, it is interesting to evaluate the influence of the weaving process on the tensile behavior of the flax-wrapped rovings. The tensile tests were performed on rovings extracted from plain and satin-manufactured fabrics for both directions (warp and weft) and at three different gauge lengths (25 mm, 50 mm, and 100 mm). Figure 17 shows the tenacity and the tensile curves for warp and weft-wrapped rovings after weaving compared to unwoven-wrapped roving (before weaving), respectively, at the three-gauge lengths. The boxplots represent the median value (with the first and third quartiles) of the tenacity of rovings. The error bars represent the maximum and minimum experimental values represented by square dots, and the dispersion is plotted as curves beside them. Irrespective of the pattern and weaving direction, a higher elongation at break is observed after the weaving process. For warp-wrapped rovings after plain weaving, the weaving process has improved the tenacity at break by 14% for 25 mm and 50 mm gauge lengths and by 10% for 100 mm gauge lengths. A significant increase in the maximum strain before roving breakage was detected. This increase can be explained by the fact that during the

opening and closing of the shed, the warp rovings are under high tension, undergoing cyclic mechanical stress. In addition, they are far from each other, so there is less friction between fibers, and therefore less fiber hanging. Indeed, when weaving, several frames for both weaves (satin and plain) were used to keep the rovings away from each other. For weft-wrapped rovings after plain weaving, the breaking tenacity is higher after weaving by 25% for 25 mm and 10% for 100 mm gauge lengths, but a slight decrease was observed for 50 mm gauge lengths. The weft roving is inserted with the shuttle through the warp shed, and a step of canning is necessary, consisting of cleaning the roving from imperfections to improve its aspect. This can lead to the untwisting of the rovings, but fortunately, these rovings are protected by the wrapping yarn. Finally, it can be noted that the weaving process has a positive impact on the rovings' tenacity in both directions. It is assumed that the cotton yarn has a positive influence on tenacity by protecting the yarns during the weaving process. Indeed, a higher elongation at break was observed for warp and weft rovings after the weaving process. During our study, it was shown that treated and untreated wrapped flax rovings have good hand weaving properties. It can be said that their tenacity was sufficient to withstand the stresses and strains experienced during the hand weaving process. According to the literature, there is no absolute minimum tenacity for linear flax structures to be woven on an industrial loom, as it depends on the specifications of each weaving application and industrial loom. In addition, fiber quality, spinning method, and twist are also important factors to consider. As a rule, higher-quality linear flax structures have a higher tenacity and are more suitable for industrial weaving applications. To the best of our knowledge, current work on the weaving of plant fiber rovings, especially wrapped rovings, for the manufacture of technical fabrics is limited.
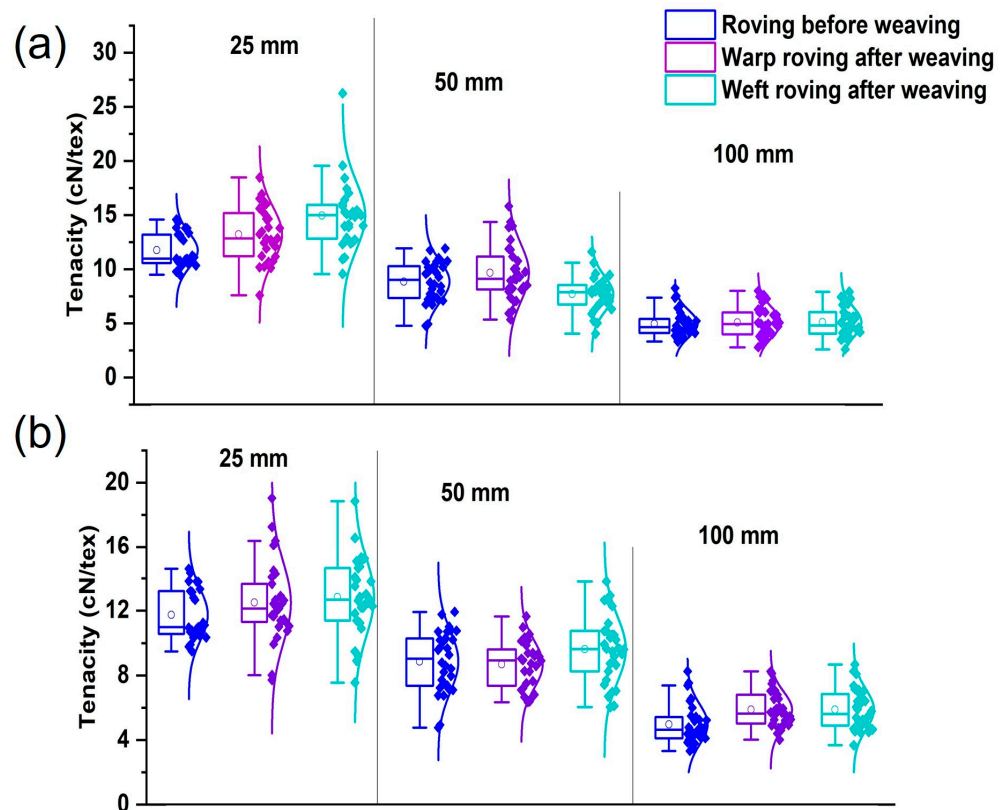
Figure 17. Breaking tenacity of rovings before weaving (blue line), warp after weaving (purple line), and weft after weaving (green line) for (**a**) plain fabric and (**b**) satin fabric (circles = median; diamonds = values).

4. Conclusions

In this study, plain and satin fabrics have been manufactured with functionalized flax rovings wrapped in cotton. These last ones have been successfully functionalized with two types of molecules: (i) quebracho tannins (Q) and (ii) 3-aminopropyltriethoxysilane (APTES) using an impregnation line. The functionalized rovings were characterized by FT-IR and observed through SEM-EDX. The presence of silane was confirmed on the surface of the flax fibers with the migration of the silane molecules to the core. A silane concentration of 1 wt.% has been shown to provide rovings and fabrics with better mechanical properties, probably due to a better penetration of the silane into the fibers, compared to higher concentrations (5 wt.%). Uniaxial tensile tests revealed that the combination of NaOH and quebracho tannins on flax fibers improved the mechanical strength of the rovings and, subsequently, of the manufactured fabrics. Results show that NaOH may play a major role in functionalization efficiency. It may help open up the side chains of tannins, allowing a better reaction with flax fibers. This increases the solubility and reactivity of tannins, thereby improving the functionalization of flax fibers. The tenacity of the untreated and treated rovings was investigated at different gauge lengths, and it was observed that an increase in the gauge length decreases the tenacity of the untreated and treated rovings. Several conclusions can also be drawn at the fabric level. A concentration of 1% silane is sufficient to improve the mechanical properties of wicks and fabrics. The addition of NaOH to tannins strengthens linen fibers more than tannins alone, and the weave pattern influences mechanical performance. This effect is due to the long floats on the surface of the fabric that create a smoother surface, which induces better resistance in the weft direction. This effect is observed for all fabrics based on treated rovings. During the weaving process and for the two types of fabrics (plain and satin), even though the rovings in the warp direction are subjected to cyclic stretching, this does not lead to a decrease in breaking tenacity but to an increase in breaking elongation.

Author Contributions: Conceptualization, A.B.; methodology, A.B., D.P., C.L. and K.T.-G.; investigation, K.T.-G.; resources, K.T.-G.; writing—original draft preparation, K.T.-G.; writing—review and editing, D.P., C.L., P.-J.L., P.O., J.T., F.S. and A.B.; visualization, K.T.-G.; supervision, D.P., C.L. and A.B.; project administration, C.L.; funding acquisition, A.B. All authors have read and agreed to the published version of the manuscript.

References

1. Yan, L.; Chouw, N.; Jayaraman, K. Flax fibre and its composites—A review. *Compos. Part B Eng.* **2014**, *56*, 296–317. [CrossRef]
2. Li, M.; Pu, Y.; Thomas, V.M.; Yoo, C.G.; Ozcan, S.; Deng, Y.; Nelson, K.; Ragauskas, A.J. Recent advancements of plant-based natural fiber–reinforced composites and their applications. *Compos. Part B Eng.* **2020**, *200*, 108254. [CrossRef]
3. Bledzki, A.K.; Gassan, J. Composites reinforced with cellulose. *Prog. Polym. Sci.* **1999**, *24*, 221–274. [CrossRef]
4. Shah, D.U.; Schubel, P.J.; Clifford, M.J. Can flax replace E-glass in structural composites? A small wind turbine blade case study. *Compos. Part B Eng.* **2013**, *52*, 172–181. [CrossRef]
5. Holbery, J.; Houston, D. Natural-fiber-reinforced polymer composites in automotive applications. *J. Miner. Met. Mater. Soc.* **2006**, *58*, 80–86. [CrossRef]
6. Sanjay, M.R.; Siengchin, S.; Parameswaranpillai, J.; Jawaid, M.; Pruncu, C.I.; Khan, A. A comprehensive review of techniques for natural fibers as reinforcement in composites: Preparation, processing and characterization. *Carbohydr. Polym.* **2019**, *207*, 108–121.
7. Rangappa, S.M.; Siengchin, S. Moving towards biofiber-based composites: Knowledge gaps and insights. *Express Polym. Lett.* **2022**, *16*, 451–452. [CrossRef]
8. Baley, C.; Bourmaud, A. Multiscale Structure of Plant Fibers. *Encycl. Mater. Compos.* **2021**, *3*, 117–134.

9. Bourmaud, A.; Nuez, L.; Goudenhooft, C.; Baley, C. Multi-scale mechanical characterization of flax fibres for the reinforcement of composite materials. In *Handbook of Natural Fibres*; Woodhead Publishing: Cambridge, UK, 2020; pp. 205–226.

10. Gurunathan, T.; Mohanty, S.; Nayak, S.K. A review of the recent developments in biocomposites based on natural fibres and their application perspectives. *Compos. Part A Appl. Sci. Manuf.* **2015**, *77*, 1–25. [CrossRef]

11. Renault, T. Les Materiaux Composites Dans L'Automobile. *Mécanique et Industries* **2001**, *2*, 211–218. [CrossRef]

12. Zhu, J.; Zhu, H.; Njuguna, J.; Abhyankar, H. Recent development of flax fibres and their reinforced composites based on different polymeric matrices. *Materials* **2013**, *6*, 5171–5198. [CrossRef]

13. Baley, C.; Bourmaud, A.; Davies, P. Eighty years of composites reinforced by flax fibers: A historical review. *Comp Part A* **2021**, *144*, 106333. [CrossRef]

14. AFNOR NF T25-501-2 Reinforcement Fibres—Flax Fibres fro Platics Composites. Part 2. Determination of Tensile Properties of Elementary Flax Fibres. AFNOR Edition. 2015. Available online: https://www.boutique.afnor.org/fr-fr/norme/nf-t255012/fibres-de-renfort-fibres-de-lin-pour-composites-plastiques-partie-2-determi/fa059503/44866 (accessed on 6 February 2024).

15. Musa, C.; Kervoëlen, A.; Danjou, P.E.; Bourmaud, A.; Delattre, F. Bio-based unidirectional composite made of flax fibre and isosorbide-based epoxy resin. *Mater. Lett.* **2020**, *258*, 126818. [CrossRef]

16. Habibi, M.; Laperrière, L.; Lebrun, G.; Toubal, L. Combining short flax fiber mats and unidirectional flax yarns for composite applications: Effect of short flax fibers on biaxial mechanical properties and damage behaviour. *Compos. Part B Eng.* **2017**, *123*, 165–178. [CrossRef]

17. Torres, J.P.; Vandi, L.J.; Veidt, M.; Heitzmann, M.T. The mechanical properties of natural fibre composite laminates: A statistical study. *Compos. Part A Appl. Sci. Manuf.* **2017**, *98*, 99–104. [CrossRef]

18. Doineau, E.; Coqueugniot, G.; Pucci, M.F.; Caro, A.S.; Cathala, B.; Benezet, J.C.; Bras, J.; Le Moigne, N. Hierarchical thermoplastic biocomposites reinforced with flax fibres modified by xyloglucan and cellulose nanocrystals. *Carbohydr. Polym.* **2021**, *254*, 11740. [CrossRef] [PubMed]

19. Ouagne, P.; Soulat, D.; Hivet, G.; Allaoui, S.; Duriatti, D. Analysis of defects during the preforming of a woven flax reinforcement. *Adv. Compos. Lett.* **2011**, *20*, 105–108. [CrossRef]

20. Torres, J.P.; Vandi, L.J.; Veidt, M.; Heiztmann, M.T. Statistical data for the tensile properties of natural fibre composites. *Data Br.* **2017**, *12*, 222–226. [CrossRef] [PubMed]

21. Zhou, N.; Geng, X.; Ye, M.; Yao, L.; Shan, Z. Mechanical and sound adsorption properties of cellular poly (lactic acid) matrix composites reinforced with 3D ramie fabrics woven with co-wrapped yarns. *Ind. Crop. Prod.* **2014**, *56*, 1–8. [CrossRef]

22. Elmogahzy, Y.E. Chapter 9: Yarns. In *Engineering Textiles*; Woodhead Publishing: Cambridge, UK, 2020.

23. Corbin, A.C.; Ferreira, M.; Labanieh, A.R.; Soulat, D. Natural fiber composite manufacture using wrapped hemp roving with. *Mater. Today Proc.* **2020**, *31*, 329–334. [CrossRef]

24. Baghaei, B.; Skrifvars, M.; Berglin, L. Manufacture and characterisation of thermoplastic composites made from PLA / hemp co-wrapped hybrid yarn prepregs. *Compos. Part A* **2013**, *50*, 93–101. [CrossRef]

25. Liotier, P.J.; Pucci, M.F.; Le Duigou, A.; Kervoelen, A.; Tirillo, J.; Sarasini, F.; Drapier, S. Role of interface formation versus fibres properties in the mechanical behaviour of bio-based composites manufactured by Liquid Composite Molding processes. *Compos. Part B Eng.* **2019**, *163*, 86–95. [CrossRef]

26. Pucci, M.F.; Liotier, P.J.; Seveno, D.; Fuentes, C.; Van Vuure, A.; Draier, S. Wetting and swelling property modifications of elementary flax fibres and their effects on the Liquid Composite Molding process. *Compos. Part A Appl. Sci. Manuf.* **2017**, *97*, 31–40. [CrossRef]

27. Vo, H.N.; Pucci, M.F.; Drapier, S.; Liotier, P.J. Capillary pressure contribution in fabrics as a function of fibre volume fraction for Liquid Composite Moulding processes. *Colloids Surfaces A Physicochem. Eng. Asp.* **2022**, *635*, 128120. [CrossRef]

28. Teraube, O.; Gratier, L.; Agopian, J.C.; Pucci, M.F.; Liotier, P.J.; Hajjar-Garreau, S.; Petit, E.; Batisse, N.; Bousquet, A.; Charlet, K.; et al. Elaboration of hydrophobic flax fibers through fluorine plasma treatment. *Appl. Surf. Sci.* **2023**, *611*, 155615. [CrossRef]

29. Ramachandran, A.R.; Rangappa, S.M.; Kushvaha, V.; Khan, A.; Seingchin, S.; Dhakal, H.N. Modification of Fibers and Matrices in Natural Fiber Reinforced Polymer Composites: A Comprehensive Review. *Macromol. Rapid Commun.* **2022**, *43*, e2100862. [CrossRef]

30. Li, Z.; Zhou, X.; Pei, C. Effect of sisal fiber surface treatment on properties of sisal fiber reinforced polylactide composites. *Int. J. Polym. Sci.* **2011**, *2011*, 803428. [CrossRef]

31. Hamidon, M.H.; Sultan, M.T.H.; Ariffin, A.H.; Shah, A.U.M. Effects of fibre treatment on mechanical properties of kenaf fibre reinforced composites: A review. *J. Mater. Res. Technol.* **2019**, *8*, 3327–3337. [CrossRef]

32. Jha, K.; Kataria, R.; Verma, J.; Pradhan, S. Potential biodegradable matrices and fiber treatment for green composites: A review. *AIMS Mater. Sci.* **2019**, *6*, 119–138. [CrossRef]

33. Kabir, M.M.; Wang, H.; Lau, K.T.; Cardona, F. Chemical treatments on plant-based natural fibre reinforced polymer composites: An overview. *Compos. Part B Eng.* **2012**, *43*, 2883–2892. [CrossRef]

34. Mokhothu, T.H.; Mtibe, A.; Mokhena, T.C.; Mochane, M.J. Influence of silane modification on the properties of natural fibers and its effect on biocomposites. In *Surface Treatment Methods of Natural Fibres and their Effects on Biocomposites*; Woodhead Publishing: Cambridge, UK, 2022; pp. 67–93.

35. Xie, Y.; Hill, C.A.S.; Xiao, Z.; Militz, H.; Mai, C. Silane coupling agents used for natural fiber/polymer composites: A review. *Compos. Part A Appl. Sci. Manuf.* **2010**, *41*, 806–819. [CrossRef]

36. Arun Prakash, V.R.; Julyes Jaisingh, S. Mechanical strength behaviour of silane treated E-glass fibre, Al-6061 and SS-304 wire mesh reinforced epoxy resin Hybrid composites. *Def. Technol.* **2018**, *10*, 2279–2286. [CrossRef]
37. Wu, H.F.; Dwight, D.W.; Huff, N.T. Effects of silane coupling agents on the interphase and performance of glass-fiber-reinforced polymer composites. *Compos. Sci. Technol.* **1997**, *57*, 975–983. [CrossRef]
38. Thomason, J.L. Glass fibre sizing: A review. *Compos. Part A Appl. Sci. Manuf.* **2019**, *127*, 105619. [CrossRef]
39. Jing, M.; Che, J.; Xu, S.; Liu, Z.; Fu, Q. The effect of surface modification of glass fiber on the performance of poly(lactic acid) composites: Graphene oxide vs. silane coupling agents. *Appl. Surf. Sci.* **2018**, *435*, 1046–1056. [CrossRef]
40. Bergeret, A. Chapter 3: Surface treatments in fibre-reinforced composites. In *Fiber Reinforced Composites*; Woodhead Publishing: Cambridge, UK, 2021.
41. Reulier, M.; Perrin, R.; Avérous, L. Biocomposites based on chemically modified cellulose fibers with renewable fatty-acid-based thermoplastic systems: Effect of different fiber treatments. *J. Appl. Polym. Sci.* **2016**, *133*, 1–13. [CrossRef]
42. Sgriccia, N.; Hawley, M.C.; Misra, M. Characterization of natural fiber surfaces and natural fiber composites. *Compos. Part A Appl. Sci. Manuf.* **2008**, *39*, 1632–1637. [CrossRef]
43. Kabir, M.M.; Wang, H.; Lau, K.T.; Cardona, F. Effects of chemical treatments on hemp fibre structure. *Appl. Surf. Sci.* **2013**, *276*, 13–23. [CrossRef]
44. Calabia, B.P.; Ninomiya, F.; Yagi, H.; Oishi, A.; Taguchi, K.; Kunioka, M.; Funabashi, M. Biodegradable poly(butylene succinate) composites reinforced by cotton fiber with silane coupling agent. *Polymers* **2013**, *5*, 128–141. [CrossRef]
45. Le Moigne, N.; Longerey, M.; Taulemesse, J.M.; Bénézet, J.C.; Bergeret, A. Study of the interface in natural fibres reinforced poly(lactic acid) biocomposites modified by optimized organosilane treatments. *Ind. Crops Prod.* **2014**, *52*, 481–494. [CrossRef]
46. Georgiopoulos, P.; Kontou, E.; Georgousis, G. Effect of silane treatment loading on the flexural properties of PLA/flax unidirectional composites. *Compos. Commun.* **2018**, *10*, 6–10. [CrossRef]
47. Yu, T.; Ren, J.; Li, S.; Yuan, H.; Li, Y. Effect of fiber surface-treatments on the properties of poly(lactic acid)/ramie composites. *Compos. Part A Appl. Sci. Manuf.* **2010**, *41*, 499–505. [CrossRef]
48. Li, Y.; Hu, C.; Yu, Y. Interfacial studies of sisal fiber reinforced high density polyethylene (HDPE) composites. *Compos. Part A Appl. Sci. Manuf.* **2008**, *39*, 570–578. [CrossRef]
49. Zhou, F.; Cheng, G.; Jiang, B. Effect of silane treatment on microstructure of sisal fibers. *Appl. Surf. Sci.* **2014**, *292*, 806–812. [CrossRef]
50. Asim, M.; Jawaid, M.; Abdan, K.; Ishak, M.R. Effect of Alkali and Silane Treatments on Mechanical and Fibre-matrix Bond Strength of Kenaf and Pineapple Leaf Fibres. *J. Bionic Eng.* **2016**, *13*, 426–435. [CrossRef]
51. Hasan, A.; Rabbi, M.S.; Maruf Billah, M. Making the lignocellulosic fibers chemically compatible for composite: A comprehensive review. *Clean. Mater.* **2022**, *4*, 100078. [CrossRef]
52. Acera Fernandez, J.; Le Moigne, N.; Bergeret, A. Modification of Flax Fibres for the Development of Epoxy-Based Biocomposites: Role of Cell Wall Components and Surface Treatments on the Microstructure and Mechanical Properties. PhD Thesis, University of Montpellier, Montpellier, France, 2015.
53. Liu, X.D.; Nishi, N.; Tokura, S.; Sakairi, N. Chitosan coated cotton fiber: Preparation and physical properties. *Carbohydr. Polym.* **2001**, *44*, 233–238. [CrossRef]
54. Prabhakar, M.N.; Song, J.-I. Fabrication and characterisation of starch/chitosan/flax fabric green flame-retardant composites. *Int. J. Biol. Macromol.* **2018**, *119*, 1335–1343.
55. Dong, A.; Yu, Y.; Yuan, J.; Wang, Q.; Fan, X. Hydrophobic modification of jute fiber used for composite reinforcement via laccase-mediated grafting. *Appl. Surf. Sci.* **2014**, *301*, 418–427. [CrossRef]
56. Khanbabaee, K.; van Ree, T. Tannins: Classification and definition. *Nat. Prod. Rep.* **2001**, *18*, 641–649.
57. Falcão, L.; Araújo, M.E.M. Tannins characterization in historic leathers by complementary analytical techniques ATR-FTIR, UV-Vis and chemical tests. *J. Cult. Herit.* **2013**, *14*, 499–508. [CrossRef]
58. Hemingway, R.W. Introduction to the chemistry and significance of condensed tannins. *J. Eng. Appl. Sci.* **1996**, *2*, 1382–1386.
59. Karaseva, V.; Bergeret, A.; Lacoste, C.; Fulcrand, H.; Ferry, L. New biosourced flame retardant agents based on gallic and ellagic acids for epoxy resins. *Molecules* **2019**, *24*, 4305. [CrossRef] [PubMed]
60. Laoutid, F.; Karaseva, V.; Costes, L.; Brohez, S.; Mincheva, R.; Dubois, P. Novel bio-based flame retardant systems derived from tannic acid. *J. Renew. Mater.* **2018**, *6*, 559–572. [CrossRef]
61. Bayart, M.; Adjallé, K.; Diop, A.; Ovlaque, P.; Barnabé, S.; Robert, M.; Elkoun, S. PLA/flax fiber bio-composites: Effect of polyphenol-based surface treatment on interfacial adhesion and durability. *Compos. Interfaces* **2020**, *28*, 287–308. [CrossRef]
62. Pantoja-Castroa, M.A.; González-Rodríguez, H. Study by infrared spectroscopy and thermogravimetric analysis of Tannins and Tannic acid. *Rev. Latinoam. Quim.* **2011**, *39*, 107–112.
63. ASTM C1557-20 Standard Test Method for Tensile Strength and Young's Modulus of Fibers. 2020. Available online: https://www.astm.org/c1557-20.html (accessed on 6 February 2024).
64. AFNOR NF G07-316. Textiles—Essais des Fils—Détermination de la Masse Linéique. AFNOR Edition. 1988. Available online: https://www.boutique.afnor.org/fr-fr/norme/nf-g07316/textiles-essais-des-fils-determination-de-la-masse-lineique-resulte-de-linc/fa018845/8441 (accessed on 6 February 2024).

65. AFNOR NF EN ISO 5084. Textiles—Détermination de L'épaisseur des Textiles et Produits Textiles. AFNOR Edition. 1996. Available online: https://www.boutique.afnor.org/fr-fr/norme/nf-en-iso-5084/textiles-determination-de-lepaisseur-des-textiles-et-produits-textiles/fa036917/8323 (accessed on 6 February 2024).

66. AFNOR NF EN 12127. Textiles—Étoffes—Détermination de la Masse Surfacique sur de Petits Echantillons. AFNOR Edition. 1998. Available online: https://www.boutique.afnor.org/fr-fr/norme/nf-en-12127/textiles-etoffes-determination-de-la-masse-surfacique-sur-de-petits-echanti/fa041735/8381 (accessed on 6 February 2024).

67. Hospodarova, V.; Singovszka, E.; Stevulova, N. Characterization of Cellulosic Fibers by FTIR Spectroscopy for Their Further Implementation to Building Materials. *Am. J. Anal. Chem.* **2018**, *9*, 303–310. [CrossRef]

68. Stevulova, N.; Cigasova, J.; Estokova, A.; Terpakova, E.; Geffert, A.; Kacik, F.; Singovszka, E.; Holub, M. Properties characterization of chemically modified hemp hurds. *Materials* **2014**, *7*, 8131–8150. [CrossRef]

69. Abdelmouleh, M.; Boufi, S.; Belgacem, M.N.; Duarte, A.P.; Ben Salah, A.; Gandini, A. Modification of cellulosic fibres with functionalised silanes: Development of surface properties. *Int. J. Adhes. Adhes.* **2004**, *24*, 43–54. [CrossRef]

70. Pornwannachai, W.; Richard Horrocks, A.; Kandola, B.K. Surface Modification of Commingled Flax/PP and Flax/PLA Fibres by Silane or Atmospheric Argon Plasma Exposure to Improve Fibre–Matrix Adhesion in Composites. *Fibers* **2022**, *10*, 2. [CrossRef]

71. Garside, P.; Wyeth, P. Identification of Cellulosic Fibres by FTIR Spectroscopy: Thread and Single Fibre Analysis by Attenuated Total Reflectance. *Stud. Conserv.* **2004**, *48*, 269–275. [CrossRef]

72. Chen, K.; Xu, W.; Ding, Y.; Xue, P.; Sheng, P.; Qiao, H.; He, J. Hemp-based all-cellulose composites through ionic liquid promoted controllable dissolution and structural control. *Carbohydr. Polym.* **2020**, *235*, 116027. [CrossRef]

73. Müssig, J.; Fischer, H.; Graupner, N.; Drieling, A. Testing Methods for Measuring Physical and Mechanical Fibre Properties (Plant and Animal Fibres). In *Industrial Applications of Natural Fibres: Structure, Properties and Technical Applications*; Wiley: Hoboken, NJ, USA, 2010; pp. 267–309.

74. Arkles, B.; Goff, J. *Silanes & Silicones for Epoxy Resins*; Gelest: Morrisville, PA, USA, 2004.

75. Shan, S.; Ji, W.; Zhang, S.; Huang, Y.; Yu, Y.; Yu, W. Insights into the immobilization mechanism of tannic acid on bamboo cellulose fibers. *Ind. Crops Prod.* **2022**, *182*, 114836. [CrossRef]

76. Nam, S.; Condon, B.D.; Xia, Z.; Madison, C.A. Intumescent flame-retardant cotton produced by tannic acid and sodium hydroxide. *J. Anal. Appl. Pyrolysis* **2017**, *126*, 239–246. [CrossRef]

77. Friedman, M.; Juürgens, H.S. Effect of pH on the Stability of Plant Phenolic Compounds. *J. Agric. Food Chem.* **2000**, *48*, 2101–2110. [CrossRef]

78. Dante, M.F.; Harvey, L.P. Process for Reacting a Phenol with an Epoxy Compound and Resulting Products. US Patent US3477990A, 11 November 1969.

79. Singpee, D. *Review on Natural Dyes for Textiles from Wastes*; Samanta, A.K., Awwad, N.S., Algarni, H.M., Eds.; IntechOpen: London, UK, 2020; pp. 225–240.

80. Romhány, G.; Karger-Kocsis, J.; Czigány, T. Tensile Fracture and Failure Behavior of Technical Flax Fibers. *J. Appl. Polym. Sci.* **2003**, *90*, 3638–3645. [CrossRef]

81. Müssig, J.; Haag, K. The use of flax fibres as reinforcements in composites. In *Biofiber Reinforcements in Composite Materials*; Elsevier: Amsterdam, The Netherlands, 2015; pp. 35–85.

82. Bos, H.L.; Donald, A.M. In situ ESEM study of the deformation of elementary flax fibres. *J. Mater. Sci.* **1999**, *34*, 3029–3034. [CrossRef]

83. Sepe, R.; Bollino, F.; Boccarusso, L.; Caputo, F. Influence of chemical treatments on mechanical properties of hemp fiber reinforced composites. *Compos. Part B Eng.* **2018**, *133*, 210–217. [CrossRef]

84. Galbe, M.; Wallberg, O. Pretreatment for biorefineries: A review of common methods for efficient utilisation of lignocellulosic materials. *Biotechnol. Biofuels* **2019**, *12*, 294. [CrossRef] [PubMed]

85. Acera Fernández, J.; Le Moigne, N.; Caro-Bretelle, A.S.; El Hage, R.; Le Duc, A.; Lozachmeur, M.; Bono, P.; Bergeret, A. Role of flax cell wall components on the microstructure and transverse mechanical behaviour of flax fabrics reinforced epoxy biocomposites. *Ind. Crops Prod.* **2016**, *85*, 93–108. [CrossRef]

86. Tran, T.P.T.; Bénézet, J.C.; Bergeret, A. Rice and Einkorn wheat husks reinforced poly(lactic acid) (PLA) biocomposites: Effects of alkaline and silane surface treatments of husks. *Ind. Crops Prod.* **2014**, *58*, 111–124. [CrossRef]

87. Corbin, A.C.; Soulat, D.; Ferreira, M.; Labanieh, A.R.; Gabrion, X.; Placet, V. Multi-scale analysis of flax fibres woven fabrics for composite applications. *IOP Conf. Ser. Mater. Sci. Eng.* **2018**, *406*, 012016. [CrossRef]

88. Omrani, F.; Wang, P.; Soulat, D.; Ferreira, M. Mechanical properties of flax-fibre-reinforced preforms and composites: Influence of the type of yarns on multi-scale characterisations. *Compos. Part A Appl. Sci. Manuf.* **2017**, *93*, 72–81. [CrossRef]